and in particular to Dr. G. H. Stafford and D. C. Salter, and to Dr. L. C. W. Hobbis and all his Nimrod Division. The pion beam was shared with the University College–Westfield College group (University of London): We enjoyed a very amicable collaboration with them and wish to thank them for all their help to us. Our data were analyzed at the Atlas Computer Laboratory: We are particularly indebted to J. Sparrow and H. Hurst for help in this. We are also indebted to Mrs. J. Huxtable and her scanners in Oxford and to Dr. W. D. Walker for communicating his results to us in advance of publication.

PHYSICAL REVIEW VOLUME 156, NUMBER 5 25 APRIL 1967

New Determination of the Branching Ratios of K^+-Meson Decay in Emulsion*

POH-SHIEN YOUNG,† W. Z. OSBORNE,‡ AND WALTER H. BARKAS§
Lawrence Radiation Laboratory, University of California, Berkeley, California
(Received 3 October 1966)

A new experiment has been carried out to measure the branching ratios for K^+ decay in emulsion under improved conditions. The mesons were brought to rest in a 14-cc volume within a large stack of nuclear-research emulsion. The stack was designed so that the secondaries of the longest range could be followed to rest if they were emitted within certain cones. Some 700 such K^+ decays were chosen as the sample. The principal method for identifying the secondaries was by following the tracks to rest, thus avoiding many sources of systematic error. Ionization measurements were used to resolve ambiguities. The over-all scanning efficiency was found to be higher than 95%. The observed branching ratios for the $K_{\mu 2}$, $K_{\mu 3}$, $K_{\pi 2}$, τ, τ', and K_{e3} modes are (61.8±2.9), (5.4±0.9), (19.3±1.6), (6.0±0.4), (2.3±0.6), and (5.3±0.9)%, respectively. These results tend to reconcile the discrepancies between emulsion measurements and heavy-liquid-chamber data.

I. INTRODUCTION

THE branching ratios for the decay modes of the K^+ meson have been measured several times in the past dozen years by different research groups.[1–6] Discrepancies exist not only between data obtained by use of different kinds of detectors, but also between data obtained from similar detectors under different experimental conditions. The difference between the $K_{\mu 2}/K_{\pi 2}$ ratio obtained from the xenon bubble chamber[1,2] and from some of the early emulsion measurements[3,4] has appeared so great that it even has been put forward as evidence for a "shadow universe."[7]

To carry out our measurement of the branching ratios we have gone back, with improved techniques, to nuclear research emulsion. Track-following was employed on a scale never before undertaken. Stack size was the greatest ever used for this purpose. Better blob density was achieved and more uniform development was accomplished than in previous experiments. In addition, several new methods were introduced for the reduction of bias and for the calculation of scanning efficiencies.

It is appropriate, before describing our experiment, to review some of the previous experiments.

The two experiments performed by the Birge group[3] and Alexander *et al.*[4] have been cited[1,2,7] as providing the most precise emulsion data for the K^+ branching ratios. In Birge's pioneering experiment the sample size was moderate (149 $K_{\mu 2}$ and 77 $K_{\pi 2}$ being found for the major modes), and different batches of samples were used to determine different decay modes. Track-following, the most direct method, was employed in identifying 97 events, and blob counting at the K^+ decay point was used to determine 185 events. The stack and the sample used by Alexander *et al.* were larger, but the identification of secondaries was based almost entirely upon blob counting and scattering meas-

* Work performed under auspices of the U. S. Atomic Energy Commission.

† Present address: Physics Department, Mississippi State University, State College, Mississippi.

‡ Present address: Physics Department, Indiana University, Bloomington, Indiana.

§ Present address: Physics Department, University of California, Riverside, California.

[1] Byron P. Roe, Daniel Sinclair, John L. Brown, Donald A. Glaser, John A. Kadyk, and George H. Trilling, Phys. Rev. Letters **7**, 346 (1961).

[2] Francis S. Shaklee, Gary L. Jensen, Byron P. Roe, and Daniel Sinclair, Phys. Rev. **136**, B1423 (1964).

[3] R. W. Birge, D. H. Perkins, J. R. Peterson, D. H. Stork, and M. N. Whitehead, Nuovo Cimento **4**, 834 (1956).

[4] G. Alexander, R. H. W. Johnson, and C. O'Ceallaigh, Nuovo Cimento **6**, 478 (1957).

[5] T. E. Hoang, M. F. Kaplon, and G. Yekutieli, Phys. Rev. **102**, 1185 (1956).

[6] P. K. Aditya, J. K. Bøggild, K. H. Hansen, J. E. Hooper, and M. Scharff, in Proceedings of the Cosmic Ray Symposium Ahmedabad, India, 1960, NP-11232, p. 373 (unpublished).

[7] Allen E. Everett, Phys. Rev. Letters **14**, 615 (1965).

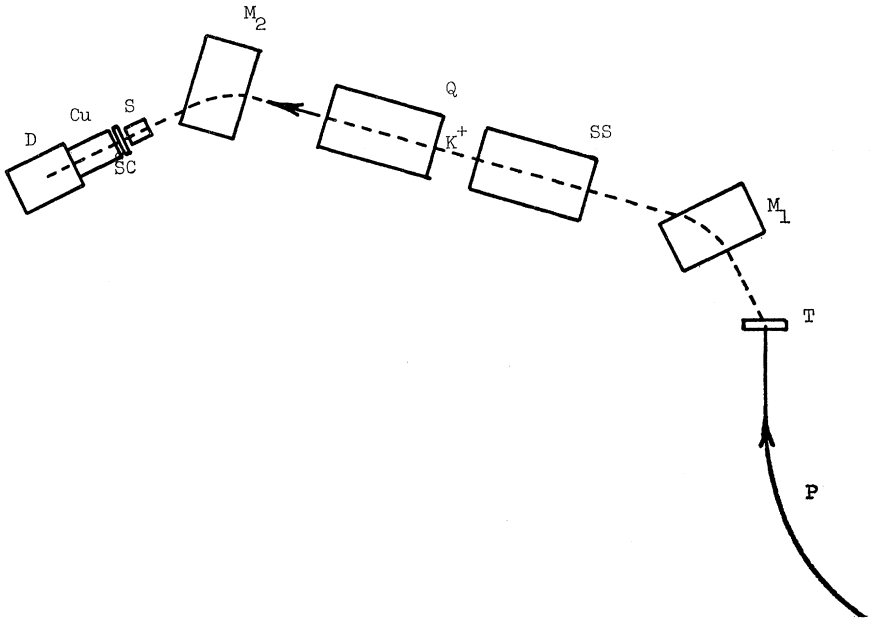

FIG. 1. Schematic diagram of exposure arrangement. P=proton beam (6.25 BeV); T=copper target; M_1=bending magnet 1; SS=static mass selector; Q=magnetic quadrupole; M_2=bending magnet 2; S=slit; SC=scintillation counter; Cu=copper moderator (12 cm); D=D-stack (15 cm thick).

urements. (Blob counting as an identification method is discussed later.) The scanning efficiencies for these two experiments were found to be the same: 100% for τ and 85% for lightly ionizing tracks.

The next two experiments to be reviewed were carried out by Roe *et al.*[1] and Shaklee *et al.*[2] with a 30-cm xenon bubble chamber. Since faster scanning is possible with bubble-chamber pictures than with emulsion plates, these two groups were able to select larger samples, which accordingly reduced the statistical fluctuations of their branching ratios (6300 K^+ mesons for Roe and 10 500 for Shaklee). Two characteristics of the xenon bubble chamber utilized by them to separate the K^+ decay modes were: (a) high efficiency for conversion of γ rays from π^0 into electron pairs, and (b) ease of recognition of electrons. However, there are ambiguities between $K_{\mu 3}$, τ', and $K_{\pi 2}$. For this reason Roe *et al.* used a kinematic test to separate $K_{\pi 2}$ from other modes. Because of measurement errors and multiple scattering of the secondary, it was found[2] that a true two-γ $K_{\pi 2}$ did not have a 100% probability of passing the test, while some of the $K_{\mu 3}$ and τ' events passed the test. The average scanning efficiencies in Roe's experiment were (85±2)% for electron pairs and (89±2.5)% for electron recognition.

In Shaklee's experiment, the kinematic test was also used but with bias corrections based on Monte Carlo calculations; this led to a lower rate for $K_{\mu 3}$ and a higher rate for $K_{\pi 2}$(see Table X). The experimental ratios of $K_{\mu 3}$ and $K_{\pi 2}$ found by Shaklee do not agree well with those of Roe. We are inclined to believe that the loss of some true $K_{\pi 2}$ events in Shaklee's experiment, when they failed the kinematic test, may have been compensated for by some $K_{\mu 3}$, $K_{e 3}$, or τ' events that passed the test. In reviewing Shaklee's experiment, two points should be mentioned: (a) the $K_{\mu 2}$ branching ratio was not measured directly, but evaluated by subtracting from 1.0 the sum of those measured for the other decay modes, (b) the probability that a τ' would be mistaken for $K_{e 3}$ was found to be (7±2)%.

On the basis of review of the previous experiments, the current measurement was planned to obtain clear-cut track identification and as large a sample size as feasible. We were able to find 4000 K^+ decays in a scan volume of 0.13 cm^3, to choose as our sample some 700 events satisfying certain geometric criteria, and to determine the decay modes with little ambiguity. Generally speaking, the results of our experiment agree better with the bubble chamber data than with the early emulsion measurements. We believe that systematic errors are largely eliminated in our experiment, owing to the ease of decay mode identification when the tracks are followed to rest. High statistical accuracy, however, especially for the minor modes, would have required an excessive effort.

II. EXPERIMENTAL PROCEDURE

A. Exposure

The D stack contains 250 Ilford K-5 emulsion pellicles, each 600 microns thick and 9×14 in.^{2} in area. The size of the stack was chosen so that when K^+ mesons come to rest and decay in the middle of the stack the secondaries (π^+ or μ^+) within certain cones can be followed from decay point to termination.

The stack was exposed to the K^+-meson beam at Berkeley. The relative positions of the various components during the exposure are shown schematically in Fig. 1. The stack was placed so that the K^+ beam was perpendicular to the surface of the pellicles and

TABLE I. Ranges of secondaries of nonrare decay modes of K^+.

Decay modes	Q (MeV)	T or T_{max} (K.E. in MeV)	R or R_{max} (range in cm in standard emulsion)
$K_{\mu 2}$	388.1	152.5	21
$K_{\mu 3}$	253.1	134.1	18
$K_{\pi 2}$	219.2	108.6	12
τ	75.0	48.1	3.5
τ'	84.2	53.2	4
K_{e3}	358.3	227.9	12[a]

[a] Electron range is poorly defined (see Ref. 8) because the straggling is large.

entered at the top of the stack (i.e., Plate No. D-250). The exposure area was about 5.3×2.5 cm^2, and more than 10^6 mesons were admitted during an exposure period of 30 h. The majority of the decays were found to have occurred in 20 consecutive plates (Plates D-126 through D-145). Therefore, we estimate that 10^6 incoming K^+ mesons stopped in a selected volume of 14 cm^3.

B. Scanning Technique

As the first step in scanning, every track that entered the stack from the upper hemisphere and stopped in the scan volume was recorded during the first area scan whether or not a secondary was found associated with it. Any event whose primary looked like a possible K^+, but for which no secondary had been found during two separate searches, was labeled no-vislble-secondary or "NVS." These events, which provided one of the bases for evaluating the over-all scanning efficiency, have been searched repeatedly for secondaries by different scanners.

It is evident that a K^+ track that stops near the top or bottom of the pellicle may not have an observable secondary if the secondary is directed towards the nearby surface. Thus, one criterion for a selected event was the incident K^+ particles must stop within the middle two-thirds of the z dimension (the depth) of the pellicle.

Since secondaries of the decay modes $K_{\mu 2}$, $K_{\mu 3}$, and $K_{\pi 2}$ may not stop in the stack unless they are emitted within certain cones, two angular intervals have been specified (as a second criterion) for the selection of events. Any secondary lying within these cones could be followed at least 14 cm, which is greater than the range of the secondary of $K_{\pi 2}$. Although the$K_{\mu 2}$ and $K_{\mu 3}$ secondaries lying in these cones sometimes do not stop in the stack, the division of events between these two classes can be carried out (see Sec. IIC). The ranges of the secondaries from nonrare decay modes of K^+ are listed in Table I.[8]

The first criterion was required for all stopping K^+ mesons; in addition, mesons having but one secondary were required to emit that secondary into one of the prescribed cones.

C. Identification of Decay Modes

The ionizing secondaries from all decay modes of the K^+ meson can be only pions, muons, or positrons. The most direct way to differentiate between these particles in emulsion is to follow the tracks to their endings and observe terminal behavior. In standard emulsion a μ particle from pion decay at rest has a characteristic range of about 600 microns, and it decays into an electron (referring to e^- or e^+) and neutrinos. Some positrons disappear through annihilation in flight, and their paths at low energy appear characteristically tortuous. We know that the ranges of the $K_{\pi 2}$ and $K_{\mu 2}$ charged secondaries are unique (21 cm for μ and 12 cm for π) because these are two-body decays. Since the range of the μ for $K_{\mu 3}$ decay can vary from 0 to 18 cm, the separation of $K_{\mu 3}$ and $K_{\mu 2}$ should present no difficulties if all secondaries are followed to rest. An analogous statement is applicable to the $K_{\pi 2}$ and τ' modes, since the maximum range of the π^+ from τ' decay is 4 cm. The τ decay mode yields three above-minimum prongs and cannot be confused with any other common mode. From the above analysis, we may conclude that the branching ratios of the nonrare decay modes of K^+ could be determined easily if all charged secondaries could be followed to their endings. However, in practice not all secondaries could be followed to their endings in spite of the proper design of the stack and the appropriate choice of the cones. Hence, ionization measurements and special analyses were also used when necessary to aid in identifying decay modes.

Our process of identification, using various methods, was as follows.

TABLE II. Decay-mode classification for DIF events.

No. of events	Identity	Method	Remarks
4	K_μ(unambiguous)	Range measurement and ionization	To be treated in Sec. IIC(e). (Two were followed to 12 cm in the second following.)
3	K_μ(probable)		
2	$K_{\pi 2}$	Range measurement and ionization	One interaction at $D=5.68$ and the other at 6.03 cm. (Both were included in SIF.)
1	K_e(probable)	Range measurement, ionization, and scattering behavior	
1	Not a K^+ decay	Recheck of the primary	The primary was a μ from a π decay and the secondary was an e.

[8] Martin J. Berger and Stephen M. Seltzer, Natl. Acad. Sci.—Natl. Res. Council, Publ. 1133, 205 (1964).

TABLE III. Decay modes of SIF events.

No. of events	Identity	Method	Remarks
17	$K_{\pi 2}$	Range measurement	Star at $D>5$ cm
21	$K_{\pi 2}$	Ionization	Star at $D<5$ cm
2	τ'	Ionization	Star at $D<5$ cm

In the first stage more than 300 of the one-prong events were followed either to their endings or as far as possible. The remainder of the one-prong events were followed only up to 12.5 cm. From the range considerations (see Table I) we know that any event with a secondary range greater than 12.5 cm could be only $K_{\mu 2}$ or $K_{\mu 3}$. The 314 events belonging to this category were labeled 12-cm events. These are treated under K_μ events in Sec. IIC.

When the first phase of track following was completed, we found that approximately 90 events had secondaries which could not be followed for 12.5 cm or to their endings. These secondaries were lost or went out of the stack in less than 12 cm (because of changes in their path directions), disappeared in flight (DIF), or produced stars in flight (SIF). The DIF events, SIF events, lost or out-of-stack (LOS) events, and K_{e3} events are treated in the following subsections: (*a*), (*b*), (*c*), and (*d*), respectively. Also given in subsec. (*b*) is a brief discussion of the use of ionization measurements.

(*a*) *DIF Events*

There were 11 events in this category as a result of the first track-following. The primaries and secondaries of these 11 apparent DIF events have been rechecked with great care by different scanners. As a result only one of them remains in the DIF category. The secondary of the remaining DIF event has been refollowed and its scattering behavior indicates it is probably an e^+. Ionization measurements and further following resolved the rest of the events. The classification of the original DIF events is shown in Table II.

(*b*) *SIF Events*

This category contained 40 interactions of which 17 had stars at $D>5$ cm ($D=$ the distance from K^+ decay point). Among all secondaries of K^+ decay the pion is the only particle that is strongly interacting and capable of producing a star in flight. Therefore this category can contain only $K\pi_2$ and τ' events but not τ decays since the latter are three-prong events. Furthermore, as the maximum range of a π^+ from τ' decay is 4 cm, only 23 SIF events can be candidates for both $K_{\pi 2}$ and τ'. The ionization method was used to resolve these events. We obtained calibration curves (see Fig. 5, Appendix I), which relate blob density (in blobs/100 μ) to residual range, according to the procedures elaborated in Appendix I. Blob counts were compared with these curves in order to effect the unambiguous resolution of all 23 SIF events which had stars at $D<5$ cm. The disposition of the 40 SIF events is given in Table III.

(*c*) *LOS Events* (*Lost or Out-of-Stack Events*)

Thirty-five tracks belonged to this class. Although the lost events have been rechecked very carefully there remain some whose secondaries still cannot be followed 12.5 cm or to their endings. Their identities have been determined as shown in Table IV.

(*d*) K_{e3} *Events*

There are two possible reasons why an event originally classified as K_{e3} may not be a true K_{e3}: (i) the primary is a μ, or (ii) an error made during the first track-following led from the true secondary track to an $e^\pm$ track. In order to minimize the possibility of making errors in the identification of these events, two steps have been taken—all primaries were followed back, and all secondaries were independently refollowed.

Although the exposure was arranged so that only the K^+ component of the beam would stop in the stack, K decays occurred upbeam from the scan volume. In this case, the secondary usually would be μ or π (which in turn decays into μ). Therefore, we should not be surprised if some $\mu \rightarrow e$ events were mistaken for $K \rightarrow e$ events. For this reason all the primaries of the 62 events originally classed asK_{e3} were studied. The result showed that 12 of these were $\mu \rightarrow e$ decays.

The second possibility for error stems from the fact that in all nonrare K^+ decay modes except $K_{\mu 2}$ and τ, at least one of the secondaries is a π^0 which decays into either two photons, or one photon and one Dalitz pair, or two Dalitz pairs. In other words, since about $30\pi^0$'s are produced per $100K^+$ decays, there are about 60 photons per 100 K^+ decays. Assuming that the average energy of the photons from π^0 decay is about 100 MeV (67.5 MeV in π^0 rest frame), we calculate that the corresponding mean free path for pair production in emulsion by these photons is approximately 5 cm.[9] This means

TABLE IV. Decay modes for LOS events.

No of events	Identity	Method	Remarks
7	$K_{\pi 2}$(unambiguous)	Ionization, range and observation behavior at end	
1	$K_{\pi 2}$(probable)		
20	K_μ(unambiguous)	Ionization and range	Treated in Sec. IIC(*e*)
6	K_μ(probable)		
1	Unresolved		

[9] Walter H. Barkas, *Nuclear Research Emulsions* (Academic Press Inc., New York, to be published), Vol. II, Chap. 5.

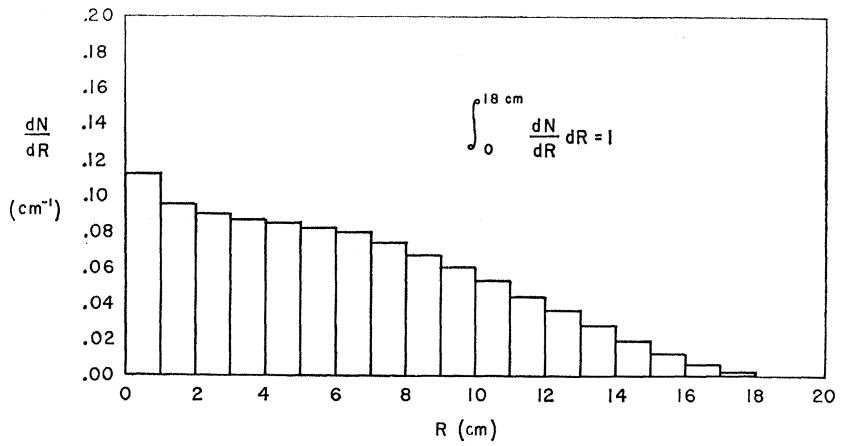

FIG. 2. Range spectrum for muons from $K_{\mu 3}$.

that almost all photons from π^0 decay convert into electron pairs in the stack. Therefore, for every 100 K^+ decays in the stack, about 120 $e^\pm$ tracks are produced. Almost all of these $e^\pm$ tracks point generally back toward the scan volume, which is very small compared with the whole stack. It is therefore estimated (details given in Appendix II) that, given a follow-through error, one has a probability of at least 40% of being led to an electron (or positron) track. This reasoning demonstrated the necessity of refollowing all secondaries of the remaining K_{e3} events. Accomplishment of this task revealed that 14 of the original K_{e3} events were, in fact, so classified because of errors in the first follow through. The disposition of all events originally classified as K_{e3} is shown in Table V.

(e) K_μ Events

There are 359 K_μ events, of which 314 are 12-cm events and 45 originally labeled LOS, DIF, or K_{e3} events. The secondary of each of these has not been followed to rest but was identified as a μ from either a range measurement or a combined range and ionization measurement. We still, however, needed to determine how many of them belong to the $K_{\mu 3}$ mode. This was accomplished by use of the known energy spectrum[10–12] of the $K_{\mu 3}$ and the number of $K_{\mu 3}$ events in which the μ^+ was observed to decay at rest. Since ranges were measured directly, we have converted the energy spectrum to a range spectrum by use of Fig. 4 for the muons from $K_{\mu 3}$ decay. A histogram of this range spectrum is shown in Fig. 2. Some 10% of this area lies above 12.5 cm. From the number of $K_{\mu 3}$ events found with $R<12.5$ cm, we deduce that three additional $K_{\mu 3}$ tracks were in the 12- to 18-cm interval.

TABLE V. Disposition of events originally classified as K_{e3}.

No. of events	Identity	Method	Remarks
36	K_{e3}	Following and refollowing both primary and secondary	
12	K_π	Following and refollowing both primary and secondary	To be treated in Sec. IIC(e). (All were followed to 12 cm in the second following.)
2	$K_{\pi 2}$	Refollowing and subsequent ionization measurements	One was included in SIF ($D>5$ cm) and the other in LOS events.
12	$\mu \rightarrow e$	Following back primary	

D. Determination of Scanning Efficiency

All track endings found during the original scan and classified as possible K's were searched for a secondary on at least two different occasions by the original scanner, provided no secondary was seen during the first search. The events for which no visible secondaries were found in any of these searches were labeled no-visible-secondary (NVS) events. These have subsequently been investigated with great care in order to provide one of the two pieces of information upon which the evaluation of our scanning efficiency is based. The treatment of the NVS events is discussed in subsec. (a) below. In subsec. (b) we discuss the efficiency program. This furnished the second basis for efficiency evaluation.

(a) NVS-Events Program

Those NVS endings contained within the middle $\frac{2}{3}$ of the z dimension in their respective pellicles were again searched for secondaries. If no secondary was found to be associated with an ending, then the primary was

[10] N. Brene, L. Egardt, and B. Qvist, Nucl. Phys. **22**, 553 (1961).
[11] John L. Brown, John A. Kadyk, George H. Trilling, Remy T. Van de Walle, Bryon P. Roe, and Daniel Sinclair, Phys. Rev. Letters **8**, 450 (1962).
[12] U. Camerini, R. L. Hantman, R. H. March, D. Murphree, G. Gidal, G. E. Kalmus, W. M. Powell, R. T. Pu, C. L. Sandler, S. Natali, and M. Villani, Phys. Rev. Letters **14**, 989 (1965).

followed back to see if it belonged to the incoming K^+ beam. Finally, each residual NVS event whose primary did belong to the beam was subjected to yet another rigorous search for a secondary.

The results of this program are listed below:

1. 1070 NVS events were found to be contained in the middle $\frac{2}{3}$ of their respective pellicle depths.
2. Secondaries were ultimately observed for 382 out of the original 1070 NVS events.
3. The primaries of 684 of the original NVS events do not belong to the K^+ beam.
4. Their remain only four endings whose primary appears to belong to the incoming K^+ beam but for which no secondary was found.

From this result we conclude that virtually all the K^+ secondaries have been observed. All events with secondaries in the cones found during the course of the NVS event program have been followed through and included in our sample.

(b) *Efficiency Rescan Program*

Some appropriately chosen parts of the original scan area have been rescanned independently by different scanners who were instructed to record every track ending coming from the upper hemisphere and lying in the middle $\frac{2}{3}$ of the pellicle depth. The results were compared with the original scans to determine which endings in the same area were found in common, in the original scan only, or in the efficiency rescan only. The original scanning efficiency ϵ_0 is calculated in a conventional way. Let us assume that

N_T="true" number of K^+ decays occurring in a scan area,

N_0=number of K^+ decays found during original scan in that area,

N_r=number of K^+ decays found during rescan in the area,

and

N_c=number of K^+ decays found in common.

Then the original and rescan efficiencies for each plate are given by

$$\epsilon_0=N_0/N_T \tag{1}$$

and

$$\epsilon_r=N_r/N_T,$$

whence

$$N_T=N_0N_r/N_c. \tag{2}$$

From Eqs. (1) and (2) we can easily calculate ϵ_0. The results are listed in Table VI.

The total area covered in the original scan was 338 mm², and that covered in the efficiency rescan was 96 mm². Although each individual plate efficiency was determined from a partial rescan area, we may assume that efficiency to be applicable to the entire plate because the original scan for each plate was carried out entirely by one particular scanner. Furthermore, the rescan area was distributed evenly over the entire original scan area. By counting the K^+ decays found in the middle $\frac{2}{3}$ of each plate during the original scan, we are able to determine the over-all efficiency ϵ for this experiment. In Table VII we list all the relevant quantities.

TABLE VI. Results of efficiency rescan.

Plate number	N_c	N_0	N_r	Original scan efficiency
D-132	137	140	143	0.958
D-134	229	237	234	0.979
D-136	377	393	414	0.910
D-138	217	224	227	0.956
D-140	268	282	279	0.961

III. RESULTS

Two sections follow. In the first section we estimate the "true" branching ratios with efficiency correction. In the second section we make general remarks on this experiment and compare our results with those obtained by other groups and with some predicted values.

A. Branching Ratios of the K^+ Decays

(a) *Observed Branching Ratios*

The selection of each one-prong event was based on the emission direction of the secondary. However, this criterion cannot be applied directly to the τ events, since these are three-prong events. By assuming that K^+ decays isotropically, we can write

$$N_{1c}/N_{1T}=N_{3c}/N_{1T}, \tag{3}$$

TABLE VII. Determination of over-all efficiency for the experiment.[a]

	N_j			
Plate number	One-prong events	Three-prong events (τ mode)	ϵ_j	N_j/ϵ_j
D-132	348	19	0.958	383.1
D-134	1248	72	0.979	1348.3
D-136	1019	58	0.910	1183.5
D-138	558	48	0.956	633.9
D-140	641	47	0.961	716.7

$$\Sigma N_j=N_{1p}+N_{3p}=3814+244=4058,$$
$$\Sigma(N_j/\epsilon_j)=4266,$$
$$\epsilon=\Sigma N_j/\Sigma(N_j/\epsilon_j)=0.951.$$

[a] Notations: N_j=number of possible K^+ decays found in the middle $\frac{2}{3}$ of the depth in plate number j. ϵ=over-all scanning efficiency for the experiment. N_{1p}=total number of one-prong events found in the middle $\frac{2}{3}$ (includes Dalitz-pair events). N_{3p}=total number of three-prong events found in the middle $\frac{2}{3}$.

TABLE VIII. One-prong events within the cones.

Decay mode	Event type: Decay at rest	LOS or 12-cm events	SIF ($D<5$ cm)	($D>5$ cm)	DIF	Scattering at end of follow-through	N_i (No. of events)
$K_{\mu 2}$	71	356					427
$K_{\mu 3}$	35	3					38
$K_{\pi 2}$	88	8	19	19			134
τ'	15		2				17
K_{e3}					1	36	37
Misc.							27[a]+1[b]
			$N_{1C}=\sum N_i=681$				

[a] One-prong events but not K^+ decay. Included in N_{1C} because the values of N_i listed in Table VIII refer to number of one-prong events found in the first area scan. Some of these are μ-e decays, etc., rather than K^+ decays.
[b] Unresolved event.

where

N_{1T} = total number of one-prong events found in the middle $\frac{2}{3}$,

N_{1c} = number of one-prong events lying within the cones,

N_{3c} = number of three-prong events to be associated with the cones (namely, number of τ events to be used in this branching ratio experiment),

and

N_{3T} = total number of three-prong events found in the middle $\frac{2}{3}$.

To solve Eq. (3), we list the experimental data concerning the one-prong events in Table VIII. By combining the information listed in Tables VII and VIII, we are able to solve Eq. (3) for N_{3c} (or N_τ). We find

$$N_{3c}=244\times(681/3814)=43.6, \tag{4}$$

or

$$N_\tau=43.6. \tag{5}$$

With N_τ evaluated, we can calculate the uncorrected branching ratios. These are listed in Table IX.

TABLE IX. Uncorrected branching ratios.

Decay mode	N_i (No. of events)	r_i (branching ratio in %)
$K_{\mu 2}$	427.1	61.31
$K_{\mu 3}$	37.9	5.44
$K_{\pi 2}$	134	19.24
τ	43.6	6.26
τ'	17	2.44
K_{e3}	37	5.31
	$\sum N_i=696.6$	$\sum r_i=100.00\%$

(b) *Corrected Branching Ratios*

Two items need to be considered in making corrections to the branching ratios listed in Table IX. The first one is related to the partial efficiencies for finding examples of different K^+ decay modes. The second one involves possible errors in following secondaries. It is convenient to deal with the second item first because the discussion requires only two short paragraphs.

In Appendix II, we have estimated that the probability of a follow-through error, if any, leading to an $e^\pm$ track as opposed to a π or μ track was at least 40%. For this reason, we had all the original K_{e3} events refollowed independently.

This demonstrated that fourteen of these events were not K_{e3}. The maximum number of possible errors in the first following is then estimated to be $14/0.4=35$. In other words, there could remain possibly 21 events in which the original track was lost and another picked up. However, the new tracks will be found in the correct π/μ ratio so that no net error is made, especially since 21 is a small number compared with the whole sample.

The difference in the partial efficiencies for different K^+ decay modes stems from the fact that each mode has a different energy spectrum, which in turn leads to different spectra as functions of blob density. We estimate that a π track with kinetic energy less than 25 MeV (corresponding to ionization greater than 38.6 blobs/100 microns in the D stack) can probably not be missed. In other words, we assume any secondary with ionization equal to or larger than 38.6 blobs/100 microns can be observed with efficiency 100%. For any secondary with ionization lower than 38.6 blobs/100 microns the efficiency will decrease with no definite relationship known to us. As the simplest approximation, we assume that the relationship is linear, i.e., the efficiency ϵ_i can be expressed as a linear function of blob density B_i,

$$\begin{aligned}\epsilon_i&=1-m(B_{25}-B_i) \quad \text{for} \quad B_i<B_{25}\\ &=1 \qquad\qquad\quad \text{for} \quad B_i>B_{25},\end{aligned} \tag{6}$$

where m is to be determined, B_i refers to a particular blob density corresponding to E_i, and B_{25} represents the blob density corresponding to a 25-MeV pion. The quantity ϵ_i is defined by

$$N_i/\epsilon_i=N_i', \tag{7}$$

where N_i = observed number of events belonging to the ith decay mode and N_i' = "true" number of events belonging to the ith mode.

Since the $K_{\mu 2}$ and $K_{\pi 2}$ secondaries have unique energies, we can apply Eq. (6) directly to these two modes to obtain [see Appendix I for the values of $B_{\mu 2}$ and $B_{\pi 2}$]

$$\epsilon_{\mu 2}=1-m(B_{25}-B_{\mu 2})=1-21.44m, \tag{8}$$

and

$$\epsilon_{\pi 2}=1-m(B_{25}-B_{\pi 2})=1-18.45m. \tag{9}$$

The $K_{\mu 3}$, K_{e3}, and τ' modes have continuous spectra. Thus, for these modes we must define their mean efficiencies:

$$\bar{\epsilon}_{\mu 3}=\int_{B\min}^{B_{25}}[1-m(B_{25}-B)]\frac{dN}{dB}dB+\int_{B}^{B\max}\frac{dN}{dB}dB, \quad (10)$$

$$\bar{\epsilon}_{e3}=\int_{B\min}^{B\max}[1-m(B_{25}-B)]\frac{dN}{dB}dB, \quad (11)$$

and

$$\bar{\epsilon}_{\tau'}=\int_{B\min}^{B_{25}}[1-m(B_{25}-B)]\frac{dN}{dB}dB+\int_{B25}^{B\max}\frac{dN}{dB}dB, \quad (12)$$

where $(dN/dB)dB$ = normalized number of events whose secondaries have a blob density lying between B and $B+dB$ at the K^+ decay point.

Since the efficiency for a three-prong event was found to be approximately 100%, we thus can write down the following equation:

$$N_\tau=N_\tau'. \quad (13)$$

By using the definition of the over-all scanning efficiency ϵ for the experiment [see Table VII], we may relate ϵ to the various ϵ_i as follows:

$$\frac{\sum N_i}{\epsilon}=\sum N_i'=\frac{N_{\mu 2}}{\epsilon_{\mu 2}}+\frac{N_{\mu 3}}{\epsilon_{\mu 3}}+\frac{N_{\pi 2}}{\epsilon_{\pi 2}}+N_\tau+\frac{N_{\tau'}}{\bar{\epsilon}_{\tau'}}+\frac{N_{e3}}{\bar{\epsilon}_{e3}}. \quad (14)$$

The corrected branching ratios are then defined by

$$r_i'=N_i'(\sum N_i'). \quad (15)$$

To solve Eq. (14) for the parameter m, we first have to calculate $\bar{\epsilon}_{\mu 3}$, $\bar{\epsilon}_{e3}$, and $\bar{\epsilon}_\tau$. Note that

$$\frac{dN}{dB}dB=\frac{dN}{dT}\frac{dT}{dB}dB, \quad (16)$$

where T refers to the kinetic energy. Equation (16) can be evaluated for $K_{\mu 3}$ by use of the energy spectrum[10–12] and Figs. 2, 4, and 5. Expression (16) can be evaluated similarly for τ' by use of the π^+ energy spectrum[13,14] and Figs. 4 and 5. But $\bar{\epsilon}_{e3}$ is obtained in Appendix II. The results of the calculations are given in Table X.

TABLE X. Partial efficiencies and corrected branching ratios.

Decay mode	ϵ_i Partial efficiency (%)	N_i'[a] ("true" number)	r_i' (corrected branching ratio in %)
$K_{\mu 2}$	94.46	452.15±21.26	61.75±2.90
$K_{\mu 3}$	96.39	39.32± 6.27	5.37±0.86
$K_{\pi 2}$	95.03	141.01±11.88	19.26±1.62
τ	100.00	43.60± 2.79	5.95±0.38
τ'	99.34	17.11± 4.14	2.34±0.57
K_{e3}	94.62	39.10± 6.25	5.34±0.85
		$\sum N_i'=732.29$	$\sum r_i'=100.00$

[a] $\Delta N_i'=(N_i')^{1/2}$ for all decay modes except τ; $\Delta N_\tau'=(N_{\tau'\text{total}})^{1/2}(681/3814)$ [see Eq. (4)].

TABLE XI. Branching ratios (%) in K^+ decay measured by different groups.

Decay mode	Emulsion: Birge *et al.*[a] (1956)	Emulsion: Alexander *et al.*[b] (1957)	Emulsion: This experiment	Xenon bubble chamber: Roe *et al.*[c] (1961)	Xenon bubble chamber: Shaklee *et al.*[d] (1964)
$K_{\mu 2}$	58.5±3.0	56.9±2.6	61.8±2.9	64.2±1.3	63.0±0.8
$K_{\mu 3}$	2.8±1.0	5.9±1.3	5.4±0.9	4.8±0.6	3.0±0.5
$K_{\pi 2}$	27.7±2.7	23.2±2.2	19.3±1.6	18.6±0.9	22.4±0.8
τ	5.6±0.4	6.8+0.4	6.0±0.4	5.7±0.3	5.1±0.2
τ'	2.1±0.5	2.2±0.4	2.3±0.6	1.7±0.2	1.8±0.2
K_{e3}	3.2±1.3	5.1±1.3	5.3±0.9	5.0±0.5	4.7±0.3

[a] Reference 3. [b] Reference 4. [c] Reference 1. [d] Reference 2.

B. Discussion of Results

(a) Comments

Our conclusions can be summarized as follows:

(i) Since the majority of the events in this experiment were identified by track-following, practically no ambiguity exists between K_μ and K_π events, between $K_{\mu 2}$ and $K_{\mu 3}$ events, or between τ' and $K_{\pi 2}$ events.

(ii) Since both the over-all and partial efficiencies were found to be high (see Tables VII and X), only a very few K^+ primaries and secondaries within the scan volume were not observed.

(iii) Although the estimate made in Appendix II of the total number of $e^\pm$ tracks produced around the scan volume was a rough approximation, it has provided a rational basis for the calculation of possible errors in track following. This estimate, combined with the careful treatment of the original K_{e3} events, has led to the conclusion that our branching ratios reflect no significant errors due to mistakes in track following.

(iv) We believe the most important conclusion of this experiment is that there remain no significant and

TABLE XII. Comparison of the data with some predicted values.

Branching ratios	Measured value	Predicted value	Underlying theory
$K_{\mu 2}$	0.618±0.029	0.677±0.011	Universality[a]
		0.69	S-wave K-π resonance[b]
$K_{\mu 3}/K_{e3}$	1.00±0.23	0.64	P-wave K-π resonance[b]
τ'/τ	0.39±0.10	0.325	$\Delta I=\frac{1}{2}$ rule[c]

[a] References 2 and 15. [b] Reference 16. [c] Reference 17.

[13] George E. Kalmus, Anne Kernan, Robert T. Pu, Wilson M. Powell, and Richard Dowd, Phys Rev. Letters **13**, 99 (1964).

[14] Douglas E. Greiner, Ph.D. thesis, Lawrence Radiation Laboratory Report No. UCRL-16058, 1965 (unpublished).

unreconciled differences between the bubble chamber and emulsion results.

(b) *Comparison*

We list five sets of branching ratios measured by different groups in Table XI.

There are a number of theoretical predictions regarding the rates for various K^+ decay modes. Table XII contains comparisons of some of our results with predicted values.[15–17]

ACKNOWLEDGMENTS

We have had many useful discussions with Frances M. Smith, Douglas E. Greiner, and Harry H. Heckman. The excellent work of our scanning and measuring staff was essential to the success of the experiment.

APPENDIX I: CALIBRATION FOR IONIZATION MEASUREMENTS

The calibration of ionization in terms of blob density was carried out for different depths in a plate, different plates in the stack, different particles, and different energies.

(a) *Blob Density with Respect to Different Depths and Different Plates*

The secondaries of ten known $K_{\tau 2}$ and ten known $K_{\mu 2}$ were so chosen that their origins were distributed over ten plates: from D-132 to D-141. The ionization along each secondary from the point of its origin was measured in terms of blob densities for a path length of about 2 mm. The blob densities were first averaged over the three portions of each plate (i.e., upper, middle, and lower portions) and then over the entire depth of each plate. Since the secondaries of the $K\tau_2$ and $K_{\mu 2}$ modes have unique energies and the loss of energy at such energies along a path of 2 mm in standard emulsion is negligible, the secondaries of each category can be considered as two monoenergetic entities which should yield two constant ionizations in a 2-mm path. Our results demonstrated that the variations with respect to depth in each plate were all smaller than ± 1 blob per 100 microns, and variations from one plate to another were even smaller. Figure 3 depicts the variation of blob density with pellicle depth. The upper curve refers to π^+ at the $K_{\tau 2}$ decay point, and the lower curve to μ^+ at the $K_{\mu 2}$ decay point.

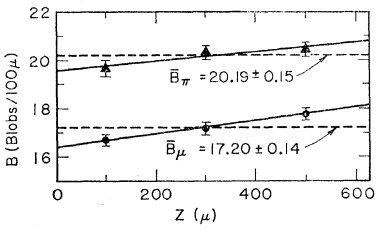

FIG. 3. Blob density as function of pellicle depth ($Z=0$ at bottom).

(b) *Kinetic Energy as a Function of Residual Range R*

Since the residual range R (rather than kinetic energy T or velocity β) is measured directly in emulsion, it is convenient to express kinetic energy as a function of R.[18] This is shown in Fig. 4.

The exact value of the mean excitation energy I for standard emulsion is at present uncertain. The old figure[18,19] of 331 eV was employed in the calculation of ionization, although there is recent evidence[20] that the best value of I is somewhat lower. The range and energy-loss rate are, however, insensitive to I, and use of the old value may be justified by noting that the ranges thus calculated agree well with the ranges of the $K_{\tau 2}$ and $K_{\mu 2}$ secondaries, which were measured incidental to this experiment.

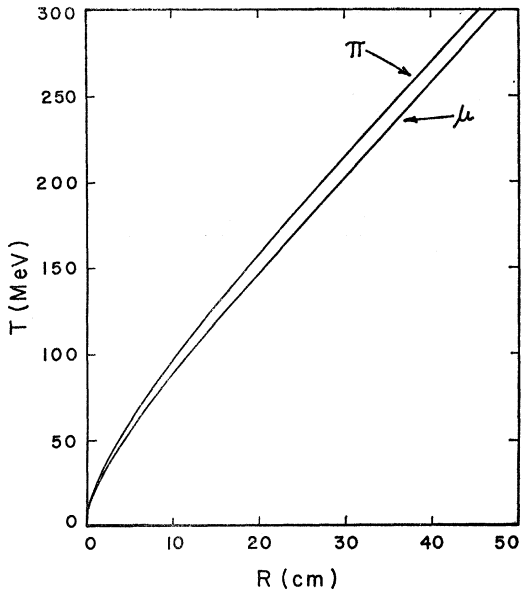

FIG. 4. Kinetic energy as function of residual range for π and μ.

(c) *Blob Density B as a Function of Residual Range R*

The blob densities of secondary tracks at different R's from known $K_{\mu 2}$ and $K_{\tau 2}$ events have been meas-

[15] Masao Sugawara (Purdue University, Lafayette, Indiana, private communication).
[16] H. Chew, Phys. Rev. Letters **8**, 297 (1962).
[17] R. H. Dalitz, Proc. Phys. Soc. (London) **A69**, 527 (1956).
[18] Walter H. Barkas, *Nuclear Researcy Emulsions* (Academic Press Inc., New York, 1963), Vol. I, Chap. 9.
[19] W. H. Barkas, P. H. Barrett, P. Cüer, H. H. Heckman, F. M. Smith, and H. K. Ticho, Nuovo Cimento **8**, 185 (1958).
[20] Walter H. Barkas and Martin J. Berger, Natl. Acad. Sci.—Natl. Res. Council Publ. **1133**, 103 (1964).

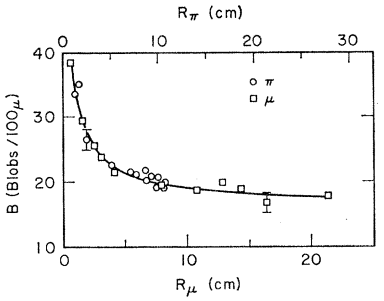

FIG. 5. Blob density as function of residual range of μ and π.

ured. The experimental data are plotted in Fig. 5 with an empirical calibration curve drawn to fit them. This curve has been used as the basis for identifying secondaries by means of ionization measurements in this experiment.

APPENDIX II: ELECTRONS IN THE EXPERIMENT

In this Appendix we elaborate the evaluation of two important quantities related to the electrons ($e^{\pm}$) in this experiment. One is the mean blob density of the e^+ tracks for K_{e3} events, and the other is the number of $e^{\pm}$ tracks produced around the scan volume in the stack.

(a) *Mean Blob Density of the e^+ Tracks for K_{e3} Events*

The partial efficiency for finding a K_{e3} was defined by Eq. (11). This can be simplified by normalizing dN/dB to unity into the form

$$\bar{\epsilon}_{e3}=1-mB_{25}+\int_{B\min}^{B\max} B\frac{dN}{dB}dB,$$

where m is to be determined.

By the definition of $(dNd/B)dB$, we can interpret the integral as follows:

$$\int_{B\min}^{B\max} B\frac{dN}{dB}dB\equiv\bar{B}\ \text{(mean blob density for the } e^+ \text{ tracks in } K_{e3} \text{ events)}.$$

The value of B can be determined by measuring the blob density of each e^+ track at the K^+ decay point for K_{e3} events and taking the average of the measurements. As the result of our blob counting for the K_{e3} events, we have obtained

$$\bar{B}=b17.81/(100\ \text{microns}). \qquad \text{(A1)}$$

By substituting Eq. (A1) and the value of B_{25} (i.e., 38.6 blobs per 100 microns) into Eq. (11), we obtain the relation between m and $\bar{\epsilon}_{e3}$.

(b) *Average Ratio between $e^{\pm}$ and $(\pi+\mu)$ Tracks Around the Scan Volume*

As the final products of all decay modes of K^+ mesons are $e^{\pm}$ and ν, it is essential to know the spatial distribution of the $e^{\pm}$ tracks in order to evaluate the number of possible errors in track following. A rough approximation is carried out below.

(*i*) *Mean energy, mean free path for the photons and $e^{\pm}$ in different decay modes.* From the energy spectra of different decay modes, we are able to list the mean energy of the π^0 and the related mean energies for photons and for electron pairs in Table XIII.

(*ii*) *Number of $e^{\pm}$ tracks per 100 K^+ mesons at different R.* As the scan volume is small compared with the whole stack, it can be considered a point source of all secondaries. Then, the number of $e^{\pm}$ tracks produced from all the modes at a distance R' from the scan volume can be expressed by

$$\begin{aligned} n_e(R')=100[&4r_{\mu 3}'(1-e^{-R'/5.04})+4r_{e3}'(1-e^{-R'/5.01})\\ &+2r'_{\pi 2}(1-e^{-R/5.00})+8r_\tau''(1-e^{-R'/6.76})\\ &+\underbrace{2r_\tau'}_{(\text{from } 2\pi^+)}+\underbrace{r_\tau''}_{(\text{from } 1\pi^+)}]. \end{aligned} \qquad \text{(A2)}$$

The increment of the $e^{\pm}$ track between R' and $R'+dR'$ is $(dn_e/dR')dR'$. Since the $e^{\pm}$ tracks cannot travel indefinitely in emulsion, we have to make corrections for this effect. For simplicity, let us suppose all $e^{\pm}$ tracks produced from all the modes had a unique range of 4.5 cm. Then we find the total number of $e^{\pm}$ tracks at different R to be

$$N_e(R)=\int_0^R H[(R'+4.5)-R]\frac{dn_e}{dR'}dR', \qquad \text{(A3)}$$

where

$$\begin{aligned} H[(R'+4.5)-R]&=1 \text{ at } R<(R'+4.5)\text{ cm},\\ &=0 \text{ at } R\geq(R'+4.5)\text{ cm}. \end{aligned} \qquad \text{(A4)}$$

After performing the numerical integration of (A3) we obtain $N_e(R)$ as a function of R. This is plotted in Fig. 6.

(*iii*) *Number of π^+ and μ^+ tracks at different R' from all modes.* By neglecting the small contribution due to

TABLE XIII. Mean energy, mean free path, and approximate range of γ and $e^{\pm}$.

Decay mode	E or $\bar{E}$ (mean energy) (MeV) π^0	γ	$e^{\pm}$	$\bar{\lambda}_\gamma$ (mean free path of γ) (cm)	$\bar{R}_e$ (approximate range of $e^{\pm}$) (cm)
$K\mu_3\rightarrow\mu\pi^0\nu$ $\pi^0\rightarrow 2\gamma\rightarrow 4e$	220	110	55	5.04	4.6
$K_{e3}\rightarrow e\pi^0\nu$ $\pi^0\rightarrow 4e$	240	120	60	5.01	4.9
$K_{\pi 2}\rightarrow\pi^+\pi^0$ $\pi^0\rightarrow 4e$ $\pi^+\rightarrow\mu^+\rightarrow e^+$	245	123	62	5.00	4.9
$\tau'\rightarrow\pi^+\pi^0\pi^0$ $\pi^0\pi^0\rightarrow 8e$ $\pi^+\rightarrow e^+$	165	83	42	6.76	3.8

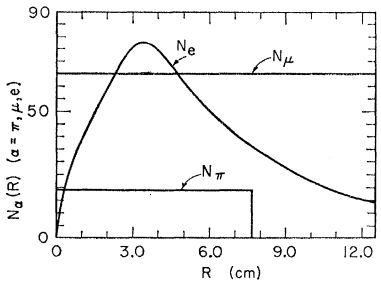

FIG. 6. Number of π, μ, and $e^{\pm}$ around scan volume as functions of distance from the volume.

τ and τ', we can estimate $N_\pi(R)$ from $K_{\pi 2}$ by considering the fact that a π track with 23 blobs per 100 microns or of a residual range ≈ 4.3 cm (i.e., 1.5 minimum ionization) is so heavily ionizing that an error involved in following such a track is very improbable. In other words, we would include a π track from $K_{\pi 2}$ for only 7.7 cm. We thus obtain

$$N_\pi(R)=r_{\pi 2}'H[7.7-R]=19.3H[7.7-R], \quad \text{(A5)}$$

where

$$H[7.7-R]=1 \text{ at } R<7.7 \text{ cm}, \quad \text{(A6)}$$
$$=0 \text{ at } R\geq 7.7 \text{ cm}.$$

For a spatial distribution of μ tracks, we include all μ tracks for both $K_{\mu 2}$ and $K_{\mu 3}$ up to 12.5 cm. We may thus write down $N_\mu(R)$ as

$$N_\mu(R)=r_{\mu 2}'+r_{\mu 3}'=61.8+5.4=67.2. \quad \text{(A7)}$$

The distributions N_π and N_μ are also plotted in Fig. 6.

(iv) Average ratio between N_e and $(N_\pi+N_\mu)$.

From Fig. 6 we can evaluate the average ratio between N_e and $(N_\pi+N_\mu)$ over a distance from $R=0$ to $R=12.5$ cm. We find

$$\int_0^{12.5 \text{ cm}} \frac{N_e(R)}{[N_\pi(R)+N_\mu(R)]}dR \Big/ \int_0^{12.5 \text{ cm}} dR=0.36. \quad \text{(A8)}$$

This underestimates the probability that a follow-through error will lead to an $e^{\pm}$ track because it does not take into account the fact that the total track density decreases approximately as $1/R^2$. Thus, the probability for making a follow-through error is considerably greater for small values of R, where $N_e/(N_\pi+N_\mu)\approx 1$. Our experience in refollowing the events originally classified as K_{e3} confirms this expectation that most errors should occur for values of R less than ≈ 7 cm. Furthermore, the inclusion of all π^+ from $K_{\pi 2}$ decay is unrealistic, because any error that led to such a track would most probably have been detected as an apparent $K_{\pi 2}$ with unreasonable pion range. Three such errors were, in fact, found and corrected during the original following. We believe that there is a probability of at least 40% that a given follow-through error will lead to an $e^{\pm}$ track.

APPENDIX III: π DECAYS IN FLIGHT

The possible number of π decays in flight among $K_{\pi 2}$ events in this experiment is evaluated here. The result shows that we may expect two or three π decays in flight. Because of the negligible effect of this number on our branching ratios, no particular effort was needed to search for such events. The evaluation is described below

Let $N_{\rm df}\equiv$No. of π's decaying in flight in a total of $N_{\pi 2}$ events. By definition, $N_{\rm df}$ can be related to $N_{\mu 2}$ by

$$N_{\rm df}=N_{\pi 2}(1-e^{-t/\tau}), \quad \text{(A9)}$$

where $N\pi_2\equiv$No. of $K_{\pi 2}$ (includes both π decaying at rest and in flight),

$t\approx(m_\pi/m_p)\times 2.84\times 10^{-9}$ sec (moderation time for a 108.6-MeV π from $K_{\pi 2}$),[21]

and

$$\tau=2.55\times 10^{-8} \text{ sec (mean life of } \pi^+).[22]$$

By approximating $N_{\pi 2}\approx 134$, we obtain

$$N_{\rm df}\approx 134(1-e^{-0.0166})=2.28. \quad \text{(A10)}$$

[21] Walter H. Barkas and D. M. Young, University of California Radiation Laboratory Report No. UCRL-2579, 1954 (unpublished).

[22] Arthur H. Rosenfeld, Angela Barbaro-Galtieri, Walter H. Barkas, Pierre L. Bastien, Janos Kirz, and Matts Roos, Rev. Mod. Phys. 36, 977 (1964).